

## Empirical M X-ray production cross sections for heavy elements by proton impact within Z-dependence analysis

Bahri DEGHFEL<sup>1,2</sup>, Farid KHALFALLAH<sup>3,4</sup>, Abdelhalim KAHOU<sup>3,4,\*</sup>, Mohammed NEKKAB<sup>1,5</sup>

<sup>1</sup>Laboratory of Materials Physics and Their Applications, Physics Department, Faculty of Sciences, University of Mohamed Boudiaf, M'sila, Algeria

<sup>2</sup>Physics Department, Faculty of Sciences, University of Mohamed Boudiaf, M'sila, Algeria

<sup>3</sup>Department of Materials Science, Faculty of Sciences and Technology, Mohamed El Bachir El Ibrahimi University, Bordj-Bou-Argeridj, Algeria

<sup>4</sup>LPMRN Laboratory, Department of Materials Science, Faculty of Sciences and Technology, Mohamed El Bachir El Ibrahimi University, Bordj-Bou-Argeridj, Algeria

<sup>5</sup>LESIMS Laboratory, Physics Department, Faculty of Sciences, Ferhat Abbas University, Setif, Algeria

Received: 26.12.2014

Accepted/Published Online: 23.06.2015

Printed: 30.11.2015

**Abstract:** New empirical M-shell X-ray production cross sections have been deduced by introducing the dependence of the universal trend of the experimental data on the atomic number of the target, noted as “Z-dependence” for semiempirical cross sections in our previous work. For this effect, the updated experimental data (from 1980 to 2009) are used to calculate the empirical cross sections for heavy elements with  $60 \leq Z \leq 90$  by proton impact. Finally, a comparison is made between the deduced results and other earlier works.

**Key words:** Empirical cross sections, Z-dependence, M-shell X-ray production cross sections

### 1. Introduction

There are different theoretical approaches developed to describe the inner shell ionization process by charged particles, namely the plan wave Born approximation (PWBA) [1], the semiclassical approximation (SCA) [2], and the classical approach, known as the binary-encounter approximation (BEA) [3] and the ECPSSR model [4,5], which is the most advanced approach based on the PWBA theory to account for energy (E) loss and Coulomb (C) deflection of the projectile and the perturbed stationary state (PSS) and relativistic (R) nature of the target's inner-shell. Despite these approaches, the theoretical predictions deviate significantly, especially at low energies, from the experimental values. This motivated us to try, after a first attempt on the semiempirical cross section [6], to deduce an empirical cross section taking into account the universal trend of the experimental data for the collective treatment [7–10] and their spread to introduce the dependence of M-shell X-ray production cross section on the atomic number of the target (Z-dependence).

In addition to the semiempirical cross sections previously calculated [6], we tried, in the present work, to investigate our previous procedure, noted as ‘Z-dependence’, to deduce new empirical M-shell X-ray production cross sections for a wide range of elements ( $60 \leq Z \leq 90$ ) by proton impact (0.1–4.0 MeV). Moreover, the present calculation was done by using the updated experimental data collected from different sources [11–20]. Then the obtained results were compared with those of other earlier works.

\*Correspondence: ka.abdelhalim@yahoo.fr

## 2. Empirical M X-ray production cross sections

Measured M X-ray production cross sections (658 data points; see Table 1 in Ref. [6]) collected from different sources [11–20] for protons energies 0.1–4.0 MeV are found to be universal when plotted, in a logarithmic scale, as a function of the scaled velocity  $\xi_M$  given as [19]

$$\xi_M = (\xi_{M_1} + \xi_{M_2} + 2\xi_{M_3} + 2\xi_{M_4} + 3\xi_{M_5})/9, \quad (1)$$

where  $\xi_s = 2v_1/\theta_s v_s$  ( $s = M_1, \dots, M_5$ ).

This is shown in Figure 1 for elements with  $60 \leq Z \leq 90$ . The universal character of M X-ray production cross sections allows us to derive an empirical cross section in the framework of the collective analysis; the set of the experimental data is fitted by a first order exponential decay function as

$$\ln(\sigma_{emp.1}) = r_0 + r_1 \exp(-r \ln \xi_M) \quad (2)$$

The fitting coefficients ( $r_0$ ,  $r_1$ , and  $r$ ) are presented in Table 1. The fitting result is shown in Figure 1 by a solid line. Moreover, as indicated in our previous work [6], the choice of the fitting functions in the present work depends only on the evolution of the distribution of the experimental data.

On the other hand, as can be seen from Figure 1, a remarkable spread is observed of the distribution of the experimental data. This fact can be exploited to introduce the Z-dependence of this distribution instead of the dependence only on the scaled velocity parameter (collective analysis). Then measured M X-ray production cross sections are presented in Figure 2 as a function of the scaled velocity parameter and the atomic number of the target ( $Z$ ). We suggest, in this work, the linear dependence on the atomic number of the distribution of the measured M X-ray production cross sections (see Figure 2). Then the previous function (Eq. (2)) becomes

$$\ln(\sigma_{emp.1}) = (r_0 + r_1 \exp(-r \ln \xi_M))(r_2 + r_3 Z), \quad (3)$$

where  $Z$  is the atomic number of the target. The fitting coefficients ( $r_0$ ,  $r_1$ ,  $r_2$ ,  $r_3$ , and  $r$ ) for the Z-dependence procedure are also presented in Table 1. The Z-dependence fits are also represented by a surface in Figure 2.

**Table 1.** Coefficients to deduce the empirical cross sections for elements with  $60 \leq Z \leq 90$  by using collective (Eqs. (2) and (4)) and Z-dependence (Eqs. (3) and (5)) procedures.

Procedure		$r$	$r_0$	$r_1$	$r_2$	$r_3$
emp.1	Collective (Eq. (2))	1.09357	8.57543	-2.92445	-	-
	Z-dependence (Eq. (3))	1.03529	-20.3593	7.28053	-0.369735	-7.77579E <sup>-4</sup>
emp.2	Collective (Eq. (4))	0.57143	27.8416	-0.77434	-	-
	Z-dependence (Eq. (5))	0.541971	5.15803	-0.163828	5.16989	3.40262 E <sup>-3</sup>

We note that the symbol emp.1 is used to denote the fitting coefficients and their corresponding calculations in the previous part. On the other hand, a plot of  $\ln(U_M^2 \sigma_M^I / Z_1)$  as a function of  $\ln(E/\lambda U_M)$  exhibits a single and approximately universal curve, where  $U_M = (U_{M_1} + U_{M_2} + 2U_{M_3} + 2U_{M_4} + 3U_{M_5})/9$  is the average binding energy of the M shell [18],  $Z_1$  and  $E$  are the charge and the energy of the projectile ( $Z_1 = 1$  for proton), respectively,  $\lambda$  is the ratio of proton mass to electron mass, and  $\sigma_M^I$  is the total ionization cross section, which is related to the total X-ray production cross section,  $\sigma_M^x$ , through  $\sigma_M^x = \bar{\omega}_M \sigma_M^I$ , where  $\bar{\omega}_M$  is the average fluorescence yield of the M-shell [21]. Figure 3 shows a plot of  $\ln(U_M^2 \sigma_M^x / \bar{\omega}_M)$  versus  $\ln(E/\lambda U_M)$  for the available

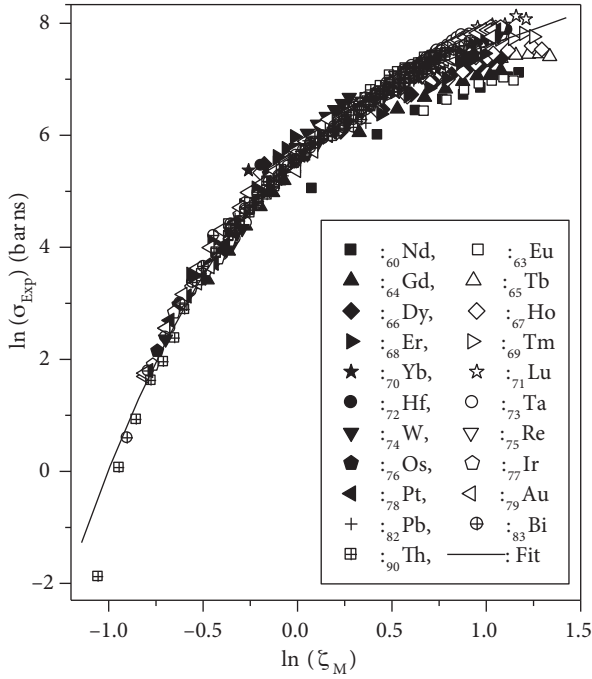


**Figure 1.** Experimental M X-ray production cross sections as a function of the scaled velocity  $\xi_M$  for elements with  $60 \leq Z \leq 90$  in a logarithmic scale. The collective fit is also represented by a solid line.

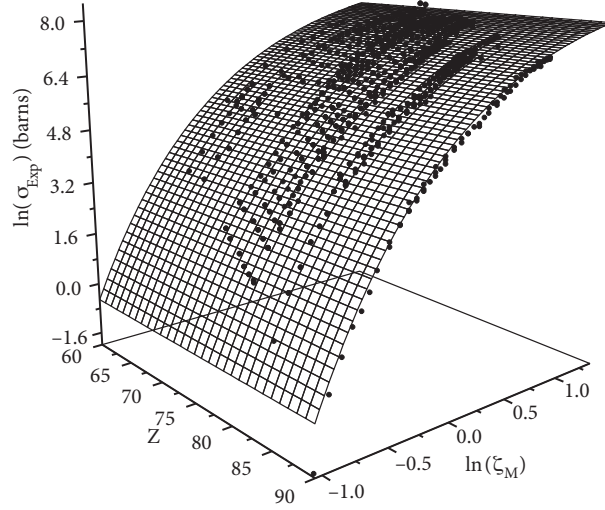


**Figure 2.** Experimental M X-ray production cross sections as a function of the scaled velocity  $\xi_M$  and the atomic number of the target ( $Z$ ) for elements with  $60 \leq Z \leq 90$ . The  $Z$ -dependence fit is also represented by a surface.

experimental data of the M-shell X-ray production cross sections for elements with  $60 \leq Z \leq 90$  (the same experimental data used in the previous part). Indeed, it can be seen that  $U_M^2 \sigma_M^x / \bar{\omega}_M$  is found to be universal when plotted in a logarithmic scaling as a function of the reduced proton energy  $E/\lambda U_M$ . Consequently, we calculate the empirical M-shell X-ray production cross sections by collective fitting the available experimental data by the same form as previously (Eq. (2)):

$$\ln(U_M^2 \sigma_{emp.2}^x / \bar{\omega}_M) = r_0 + r_1 \exp(-r \ln(E/\lambda U_M)). \quad (4)$$

Furthermore, to introduce the  $Z$ -dependence of the distribution of the experimental data ( $\ln(U_M^2 \sigma_M^I / Z_1)$  vs.  $\ln(E/\lambda U_M)$ ), in Figure 4 we plot  $\ln(U_M^2 \sigma_M^I / Z_1)$  as a function of  $\ln(E/\lambda U_M)$  and the atomic number of the target ( $Z$ ). In this work, we suggest the linear dependence on the atomic number of the cross sections ( $\ln(U_M^2 \sigma_M^I / Z_1)$ ); this allows us to fit the experimental data as follows:

$$\ln(U_M^2 \sigma_{emp.2}^x / \bar{\omega}_M) = r_0 + r_1 \exp(-r \ln(E/\lambda U_M))(r_2 + r_3 Z). \quad (5)$$

The fitting coefficients ( $r_0$ ,  $r_1$ ,  $r_2$ ,  $r_3$ , and  $r$ ) for collective analysis and the  $Z$ -dependence procedure are also presented in Table 1 (noted as emp.2). The collective and  $Z$ -dependence fits are also represented by a solid line in Figure 3 and by a surface in Figure 4, respectively.

In addition, the total deviation of the experimental cross sections ( $\sigma_{exp}$ ) from their corresponding fitted values ( $\sigma_{emp}$ ) for each element is expressed in terms of the root-mean-square error ( $\varepsilon_{rms}$ ), given by the following

expression:

$$\varepsilon_{rms} = \left[ \sum \frac{1}{N} \left( \frac{\sigma_{exp} - \sigma_{s-emp}}{\sigma_{s-emp}} \right)^2 \right]^{1/2}, \quad (6)$$

where  $N$  is the number of experimental data.

The values of  $\varepsilon_{rms}$  (%) from the calculation of the empirical cross sections for elements with  $60 \leq Z \leq 90$  by using collective (Eqs. (2) and (4)) and Z-dependence (Eqs. (3) and (5)) procedures are presented in Table 2.

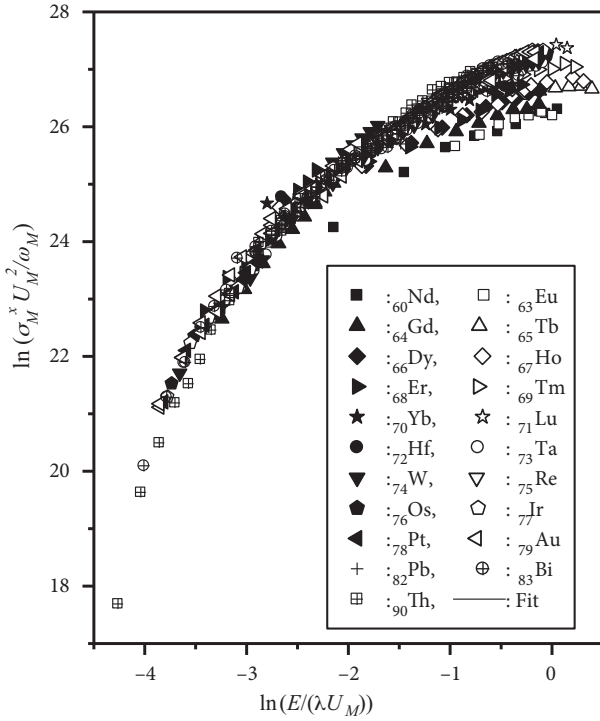


**Figure 3.** Plots of  $\ln(\sigma_M^x U_M^2 / \bar{\omega}_M)$  as a function of the reduced proton energy  $\ln(E/\lambda U_M)$  for elements with  $60 \leq Z \leq 90$  in a logarithmic scale. The collective fit is also represented by a solid line.

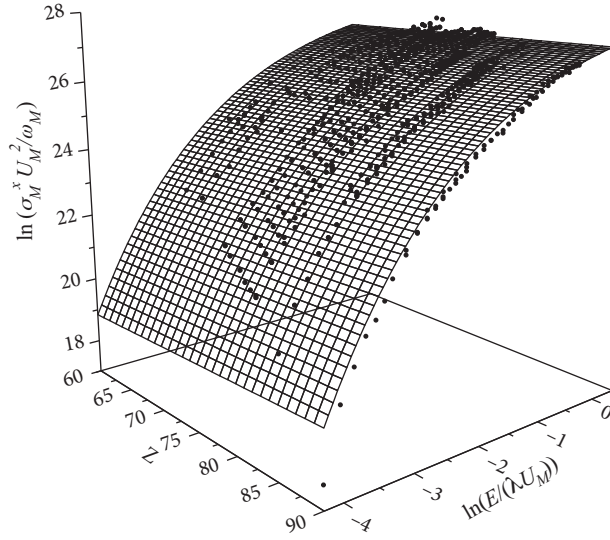


**Figure 4.** Plots of  $\ln(\sigma_M^x U_M^2 / \bar{\omega}_M)$  as a function of the reduced proton energy  $\ln(E/\lambda U_M)$  and the atomic number of the target ( $Z$ ) for elements with  $60 \leq Z \leq 90$ . The Z-dependence fit is also represented by a surface.

### 3. Results and discussion

It can be seen from Table 2 that the values of the error related to the Z-dependence procedure are either enhanced when compared to the collective procedure ones (up to 30.37% from emp.1 calculation and up to 34.44% from emp.2 for  $^{64}\text{Gd}$ ) or a slight relative deviation is observed between them, except in some cases such as  $^{68}\text{Er}$ ,  $^{69}\text{Tm}$ , and  $^{70}\text{Yb}$  for which a small number of the available experimental data are observed (6 for  $^{69}\text{Tm}$  and 9 for  $^{70}\text{Yb}$ ) or their spread, attributed to the various sources from which the experimental data have been collected, might be the reason for this deviation (for  $^{68}\text{Er}$ ).

In addition, we present, in Figure 5, our results of the empirical cross sections from both collective (Eqs. (2) and (4)) and Z-dependence (Eqs. (3) and (5)) procedures for selected elements, namely  $^{60}\text{Nd}$ ,  $^{68}\text{Er}$ ,

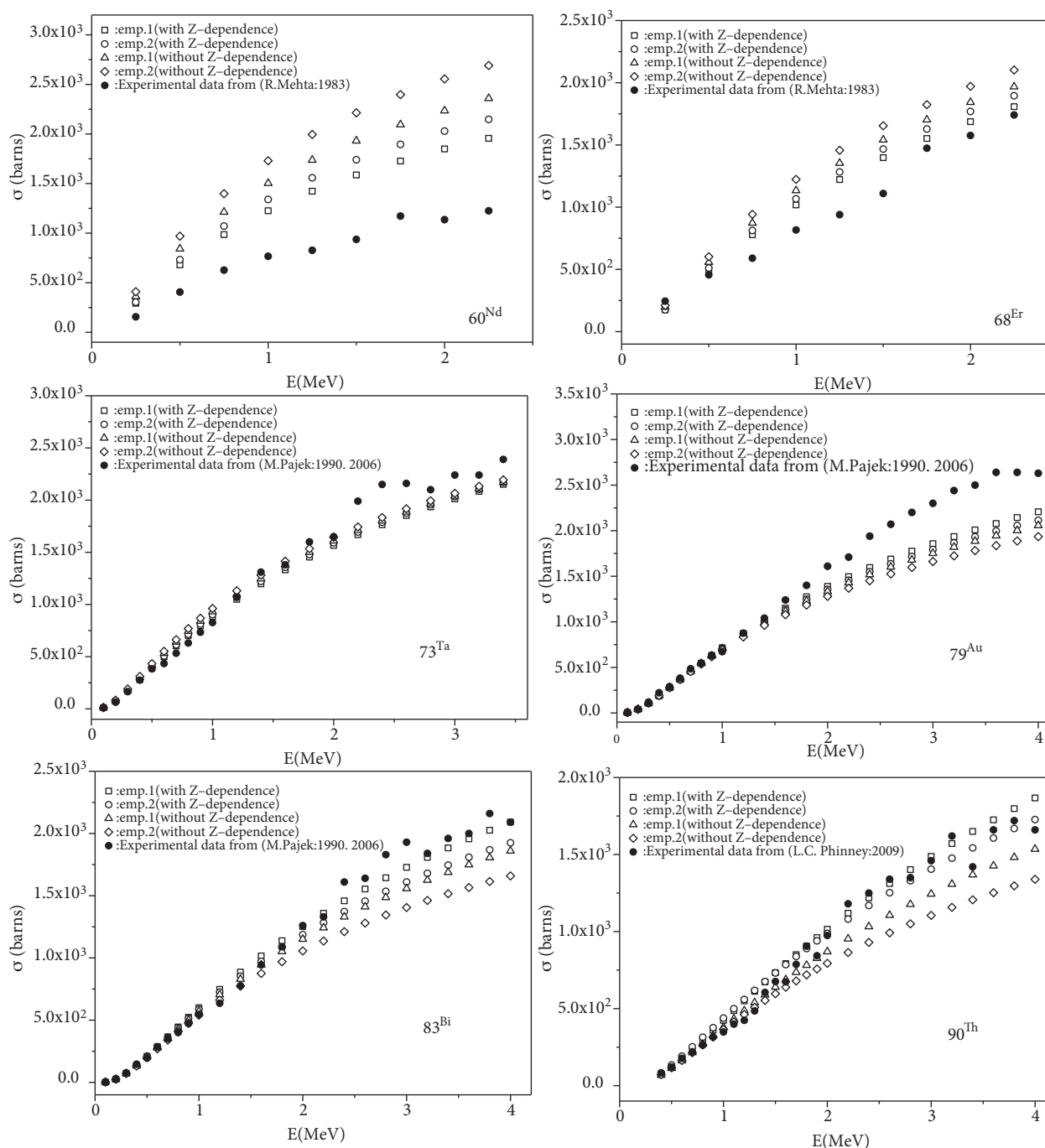


**Figure 5.** Experimental cross sections and those deduced from collective (Eqs. (2) and (4)) and Z-dependence (Eqs. (3) and (5)) procedures for selected elements as a function of proton energy.

$^{73}\text{Ta}$ ,  $^{79}\text{Au}$ ,  $^{83}\text{Bi}$ , and  $^{83}\text{Th}$ . In the same figure, we have incorporated the most recent available experimental data (Exp.) of the M-shell X-ray production cross sections for each element [13–15,20] as a function of the proton energy. Affected by the atomic number ( $Z$ ) as a parameter introduced (Eqs. (3) and (5)) in adjusting the distribution of the experimental data, the results related to the Z-dependence from both emp.1 or emp.2 procedures are close to each other (in the worst case the relative deviation between them up to 09.76% for  $^{60}\text{Nd}$ ;

**Table 2.** Root-mean-square error  $\varepsilon_{rms}$  (%) of the empirical cross sections for elements with  $60 \leq Z \leq 90$  by using collective (Eqs. (2) and (4)) and Z-dependence (Eqs. (3) and (5)) procedures.

emp.2		emp.1		Element	emp.2		emp.1		Element
Eq. (5)	Eq. (4)	Eq. (3)	Eq. (2)		Eq. (5)	Eq. (4)	Eq. (3)	Eq. (2)	
18.68	17.28	19.50	18.03	$_{73}\text{Ta}$	44.04	56.53	39.27	50.22	$_{60}\text{Nd}$
16.27	13.99	16.79	14.72	$_{74}\text{W}$	45.79	55.25	41.77	50.16	$_{63}\text{Eu}$
18.57	19.04	18.79	18.84	$_{75}\text{Re}$	22.82	34.81	20.47	29.40	$_{64}\text{Gd}$
17.25	17.70	15.20	15.86	$_{76}\text{Os}$	26.29	35.76	22.19	30.44	$_{65}\text{Tb}$
20.04	22.73	17.53	19.76	$_{77}\text{Ir}$	32.80	34.03	29.84	30.67	$_{66}\text{Dy}$
14.19	17.41	11.94	14.36	$_{78}\text{Pt}$	26.16	29.65	23.05	25.64	$_{67}\text{Ho}$
16.70	19.27	14.82	16.33	$_{79}\text{Au}$	40.45	28.23	36.49	28.65	$_{68}\text{Er}$
11.19	09.17	13.16	10.18	$_{82}\text{Pb}$	06.91	05.31	10.50	05.05	$_{69}\text{Tm}$
12.04	14.48	13.21	12.07	$_{83}\text{Bi}$	41.91	33.12	39.76	3.63	$_{70}\text{Yb}$
20.91	1.16	16.72	14.77	$_{90}\text{Th}$	41.01	34.40	45.35	39.70	$_{71}\text{Lu}$
					23.56	19.05	24.63	20.72	$_{72}\text{Hf}$

up to 04.99% for  $_{68}\text{Er}$ ; up to 11.54% for  $_{73}\text{Ta}$ ; up to 07.49% for  $_{79}\text{Au}$ ; up to 07.98% for  $_{83}\text{Bi}$ ; up to 13.15% for  $_{90}\text{Th}$ ) and they are generally much closer to the experiment ones than those related to the collective one over the whole energy range of proton.

Finally, it must be emphasized that the fitting functions (Eqs. (2)–(5)) and their associated coefficients ( $r, r_0, r_1, r_2, r_3$ ) are only valid in the region of the used experimental data (energy proton from 0.1 to 4.0 MeV and  $60 \leq Z \leq 90$ ) and their extension might deduce erroneous results, which allows us to point out the need for further works to obtain a set of parameters by using a general unique formula (Z-dependence procedure) including other groups.

#### 4. Conclusion

The available experimental data are used to deduce Z-dependence and collective empirical M-shell X-ray production cross sections for a wide range of heavy elements with  $60 \leq Z \leq 90$  by proton impact. Our results for selected heavy elements, namely  $_{60}\text{Nd}$ ,  $_{68}\text{Er}$ ,  $_{73}\text{Ta}$ ,  $_{79}\text{Au}$ ,  $_{83}\text{Bi}$ , and  $_{83}\text{Th}$ , are compared with experimental ones. The results related to the Z-dependence procedure are much closer to the experimental ones than those related to the collective one. Although both emp.1 and emp.2 Z-dependence cross sections tend generally towards the experimental data, the Z-dependence procedure by using the first method, emp.1, gives the better representation of the experimental data.

#### References

- [1] Khandelwal, G. S.; Merzbacher, E. *Phys. Rev.* **1966**, *144*, 349–352.
- [2] Garcia, J. D. *Phys. Rev. A* **1970**, *1*, 280–285.
- [3] Choi, B. H. *Phys. Rev. A* **1973**, *7*, 2056–2062.
- [4] Brandt, W.; Lapicki, G. *Phys. Rev. A* **1979**, *20*, 465–480.
- [5] Brandt, W.; Lapicki, G. *Phys. Rev. A* **1981**, *23*, 1717–1729.
- [6] Deghfel, B.; Kahoul, A.; Kerai, S.; Saadaoui, M.; Dechoucha, S.; Nekkab, M. *Radiat. Phys. Chem.* **2013**, *92*, 32–36.
- [7] Deghfel, B.; Nekkab, M.; Kahoul, A. *X-Ray Spectrom.* **2009**, *38*, 399–405.

- [8] Deghfel, B.; Kahoul, A.; Nekkab, M. *X-Ray Spectrom.* **2010**, *39*, 296–301.
- [9] Deghfel, B.; Kahoul, A.; Heraiz, S.; Belouadah, N.; Nekkab, M. *Radiat. Phys. Chem.* 2013, *85*, 89–94.
- [10] Kahoul, A.; Deghfel, B.; Abdellatif, A.; Nekkab, M. *Radiat. Phys. Chem.* 2011, **80**, 1300–1311.
- [11] Sera, K.; Ishii, K.; Yamadera, A.; Kuwako, A.; Kamiya, M.; Sebata, M.; Morita, S.; Chu, T. C. *Phys. Rev. A* **1980**, *22*, 2536–2549.
- [12] Mehta, R.; Duggan, J. L.; Price, J. L.; McDaniel, F. D.; Lapicki, G. *Phys. Rev. A* **1982**, *26*, 1883–1891.
- [13] Mehta, R.; Duggan, J. L.; Price, J. L.; Kocur, P. M.; McDaniel, F. D.; Lapicki, G. *Phys. Rev. A* **1983**, *28*, 3217–3222.
- [14] Pajek, M.; Kobzev, A. P.; Sandrik, R.; Skrypnik, A. V.; Ilkhamov, R. A.; Khumurodov, S. H.; Lapicki, G. *Phys. Rev. A* **1990**, *42*, 261–272.
- [15] Pajek, M.; Banaś, D.; Braziewicz, J.; Czarnota, M.; Bieńkowski, A.; Jaskóła, M.; Korman, A.; Trautmann, D.; Lapicki, G. *Phys. Rev. A* **2006**, *73*, 12709–12725.
- [16] Cipolla, S. J. *Nucl. Instrum. Methods B* **1995**, *99*, 22–26.
- [17] Shokouhi, F.; Fazinić, S.; Bogdanović, I.; Jakšić, M.; Valković, V.; Afarideh, H. *Nucl. Instrum. Methods B* **1996**, *109/110*, 15–18.
- [18] Rodriguez-Fernández, L.; Miranda, J.; Ruvalcaba-Sil, J. L.; Segundo, E.; Oliver, A. *Nucl. Instrum. Methods B* **2002**, *189*, 27–32.
- [19] Goudarzi, M.; Shokouhi, F.; Laméhi-Rachti, M.; Oliay, P. *Nucl. Instrum. Methods B* **2006**, *247*, 217–222.
- [20] Phinney, L. C.; Duggan, J. L.; Lapicki, G.; Naab, F. U.; Hossain, K.; McDaniel, F. D. *J. Phys. B* 2009, *42*, 085202–085210.
- [21] Söğüt, Ö.; Büyükkasap, E.; Küçükönder, A.; Ertugrul, M.; Dogan, O.; Erdogan, H.; Şimşek, Ö. *X-Ray Spectrometry* **2002**, *31*, 62–70.